

# Lab 5: X-ray Diffractometer

Otho Ulrich, Mike Pirkola, Jacob Burke, Andrew Messecar

April 17, 2017

## Abstract

Western Michigan University's new X-ray Diffractometer is used to probe four samples. The absorption depths are reported for each sample. Bragg diffraction is discussed as it pertains to a cubic geometry. The lattice constant is computed for an NaCl sample. For three amorphous samples – wood, grease, and plastic – the average distance between atoms is computed, and from this the density is computed.

## 1 Introduction

Bragg diffraction of X-rays is a useful method for characterising the atomic and molecular structure of materials. Many mechanical and electric properties are functions of the structures that constitute materials. Bragg diffraction uses the wave theory of electromagnetic radiation to predict how X-rays will interact with the atomic lattice of a crystal. The spacing between atoms can be measured by inference, and the average spacing between atoms is often called the “lattice constant”.

We attempt to compute the lattice constant from an X-ray diffractometer reading of a sample of NaCl, or common salt. NaCl forms a cubic crystal structure, so it has a single lattice constant, and this is computed from the diffraction pattern and compared to known values. Three amorphous samples are also analyzed: plastic of an unknown type; grease; and plywood. These materials are not expected to have rigid crystal structures, but the average spacing between atoms can still be ascertained from the diffraction pattern.

## 2 Bragg Diffraction

The diffraction angle of X-rays by atoms in a crystal lattice or other molecule depends on the distance between atoms. The lattice constants of a crystal describe the distances and angles between atoms, but in the case of a cubic lattice such as NaCl, there is only one relevant lattice constant. Bragg diffraction predicts strong X-ray signals at diffraction angles that produce constructive interference. Figure 1 illustrates the geometry of Bragg diffraction; the distance between planes  $d$  is the lattice constant, and the Bragg condition

$$2d \sin \theta = n\lambda, \tag{1}$$

where  $\lambda$  is the photon wavelength of the X-ray and  $n$  a positive integer describes the angles at which strong signals should be detected. [2]

The modern approach to analyzing materials by Bragg diffraction is to interpret the output as the reciprocal space representation of the lattice positions. An inverse Fourier transform then gives

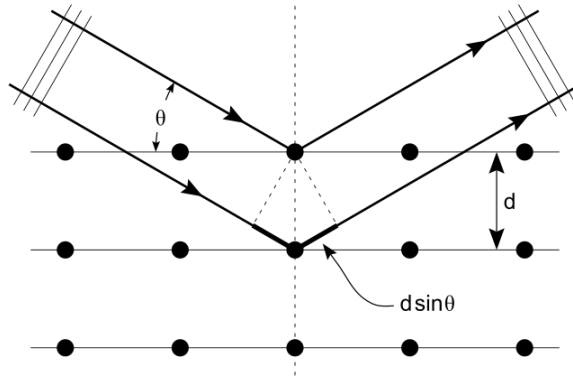


Figure 1: Bragg diffraction from a cubic crystal lattice. Plane waves incident on a crystal lattice at angle  $\theta$  are partially reflected by successive parallel crystal planes of spacing  $d$ . The superposed reflected waves interfere constructively if the Bragg condition  $2d \sin \theta = n\lambda$  is satisfied. [1]

Copper Line	Energy (eV)	Frequency (Hz)	Wavelength
K- $\alpha_1$	8046	$1.946 \times 10^{18}$	$1.541 \times 10^{-10}$
K- $\alpha_2$	8027	$1.941 \times 10^{18}$	$1.393 \times 10^{-10}$
K- $\beta$	8903	$2.153 \times 10^{18}$	$1.545 \times 10^{-10}$

the positions that make the lattice. The HighScore Plus software, associated with the Empryan XRD, is used to perform these operations. [5] It computes a spacing constant in angstroms, which can be interpreted as the cubic lattice constant, and other quantities.

A crystal powder sample will have random orientations across all possible rotations in 3 dimensions; we call this powder diffraction. In a cubic crystal the Miller indices  $(h k l)$  describe the orientation of the planes, thereby predicting a periodic lattice points along the z-axis that will produce constructive interference. While the lattice constant does not change, each orientation may result in a different diffraction spacing, so a powder diffraction will result in a diffraction pattern where signals are observed at many angles; observe Figure 2. The lattice constant can be computed in each case.

### 3 Material Structure

The structure of some samples tested here are known. Sodium-Chloride is a face-centered cubic lattice with lattice constant  $a = 564.02 pm$ . [9] This closely agrees with the value reported by Wallace and Barrett:  $a = 5.64 \pm 0.0005 \text{ \AA}$ . [10] The allowed miller indices for a FCC lattice are given in Table 1, with the computed diffraction spacing, and some of the geometries are shown in Figure 2.

Amorphous materials consisting of mostly carbon have complex structures. Therefore, they are difficult to analyze in detail. [8] The diffraction pattern peak should reach a maximum at the angle  $\theta$  corresponding to the average distance between atoms, and lesser peaks can be expected as indicators of other prominent structures within a sample. These values will be determined and a density computed from the average distance between atoms. [2]

#### 3.1 Penetration Depth

The penetration depth is computed for each material. The defining formula

$h$	$k$	$l$	$2\theta$ [°]	Spacing [Å]	Ref. Int. [%]
1	1	1	27.367	3.25626	8.7
0	0	2	31.704	2.82	100
0	2	2	45.449	1.99404	64.3
1	1	3	53.87	1.70052	2.2
2	2	2	56.474	1.62813	20.2
0	0	4	66.229	1.41	8.7
1	3	3	73.072	1.2939	1
0	2	4	75.294	1.26114	22.5
2	2	4	83.994	1.15126	16.2

Table 1: Allowed Miller indices ( $h k l$ ) for NaCl. For each, the predicted diffraction spacing along the axis normal to the sample surface is predicted, and the incidence angle with its expected reflected intensity. [10] [5]

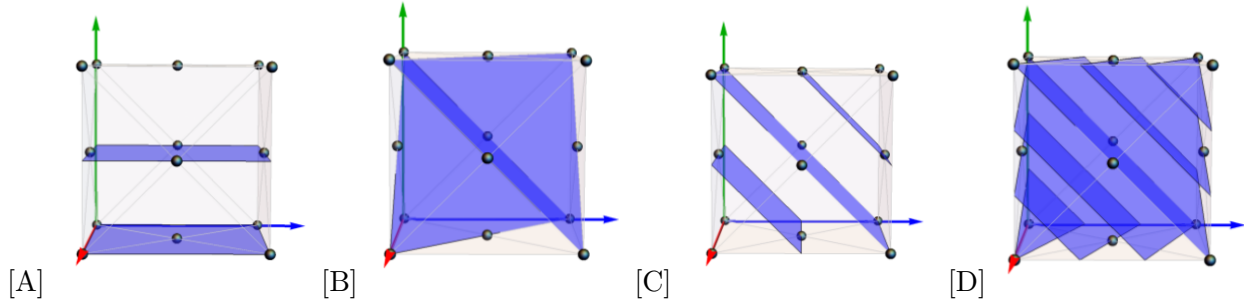


Figure 2: Four of the atomic plane orientations of a face-centered cubic lattice that result in Bragg diffraction. The Miller indices ( $h k l$ ) for each structure are [A] (0 0 2) [B] (1 1 1) [C] (0 2 2) [D] (1 3 3). The predicted diffraction spacings are tabulated in Table 1

Mat.	Packing [n.u.]	Density [g/cm <sup>3</sup> ]	MAC [cm <sup>2</sup> /g]	Pen. Depth [ $\mu m$ ]
NaCl	0.7	2.165	73.7	206
Plastic	0.6	2.0	4.3	4460
Grease	0.6	2.0	4.3	4460
Wood	0.6	2.0	4.3	4460

Table 2: Properties of interest for the materials analyzed in this study. Values for the amorphous materials are assumed to be those of simple amorphous carbon. Packing efficiencies are rough estimates. The mass attenuation coefficients are taken from the NIST Hubbell and Seltzer database, and other values are as reported on wikipedia, April 17, 2017. [4] [9] [3]

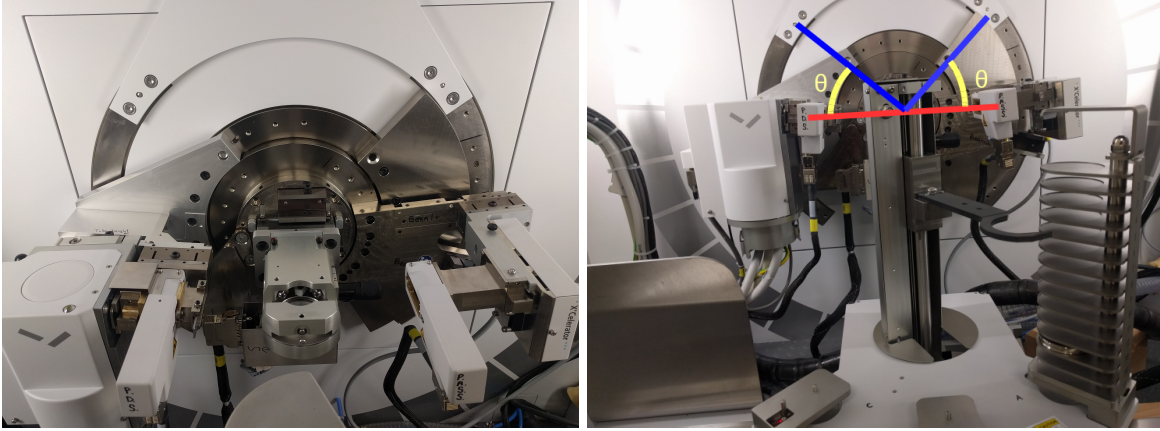


Figure 3: The PANalytical Empyrean X-ray diffractometer. Sample are placed in a bin at the center. X-rays are generated in the arm on the left, diffracted by the sample at the center, and detected at an angle  $\theta$  by the X'Celerator in the arm on the right. Each scan ran through  $\theta = \{5^\circ..45^\circ\}$ .

$$I_L = I_0 \times e^{-\left(\frac{\mu}{\rho}\rho L\right)} \quad (2)$$

is valid for symmetric (gonio) scans. [5] The HighScore Plus software computes the penetration depth from the mass attenuation coefficient, specific gravity of the material, and a powder packing efficiency. These values are tabulated in Table 2 along with the computed penetration depths. Penetration depth is computed for an incidence angle  $90^\circ$ , which gives maximum penetration.

## 4 X-ray Diffractometer

An Empyrean X-ray diffractometer by PANalytical [6] was used to collect a diffraction pattern from each sample. In this machine, an X-ray source emits onto a material sample, and a detector records X-rays diffracted at the angle of incidence; see Figure 3. X-rays are created by accelerating electrons toward a copper anode (Figure 4). The X'Celerator detector is an X-ray sensor with a window size of  $9\text{mm} \times 15\text{mm}$  and Copper K- $\alpha$  efficiency  $> 94\%$  [7].

### 4.1 Computational Details

The phases of the X-rays are not known, so the HighScore Plus software from PANalytical determines the phase by fitting predicted profiles. A background is determined using the minimum 2nd derivative method with “bending factor” = 5, “granularity” = 20, and using smoothed input data. Peaks are located with “minimum significant” = 10.00, “minimum tip width” = 0.01, “maximum tip width” = 1.00, and “peak base width” = 2.00. [5]

## 5 Results

The observed diffraction pattern from NaCl is presented in Figure 5. The HighScore software was able to identify the copper Bragg diffraction pattern, which was prominent.

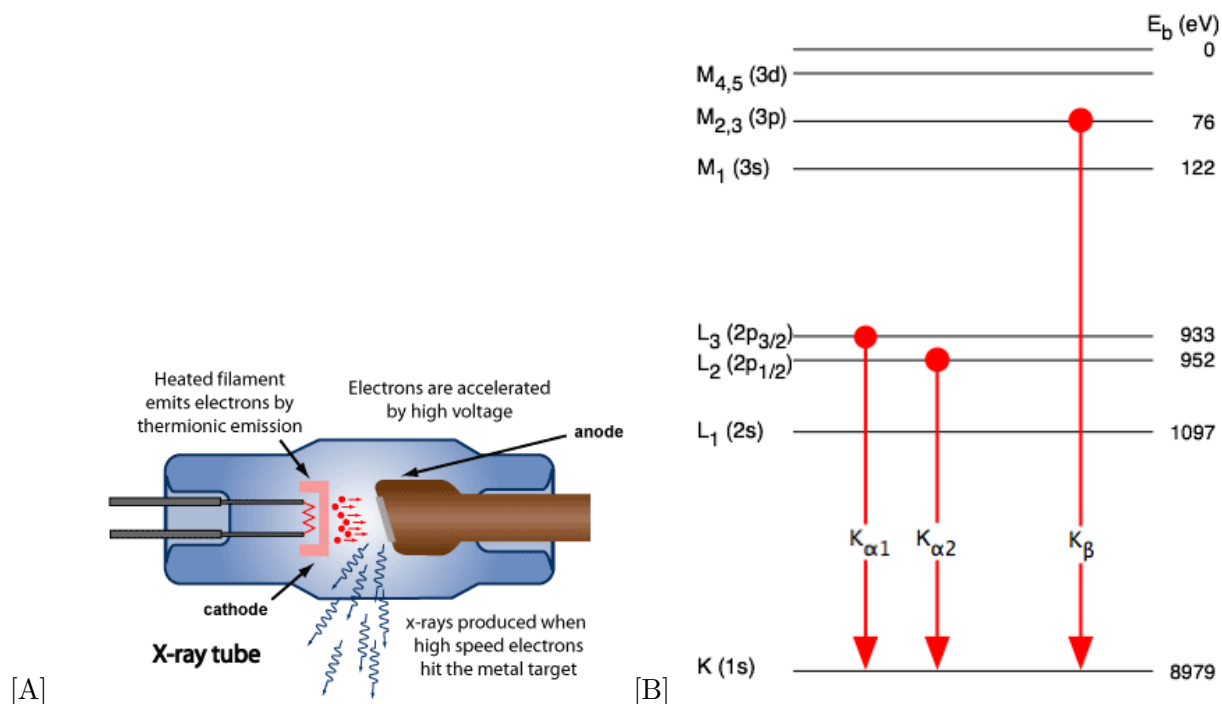
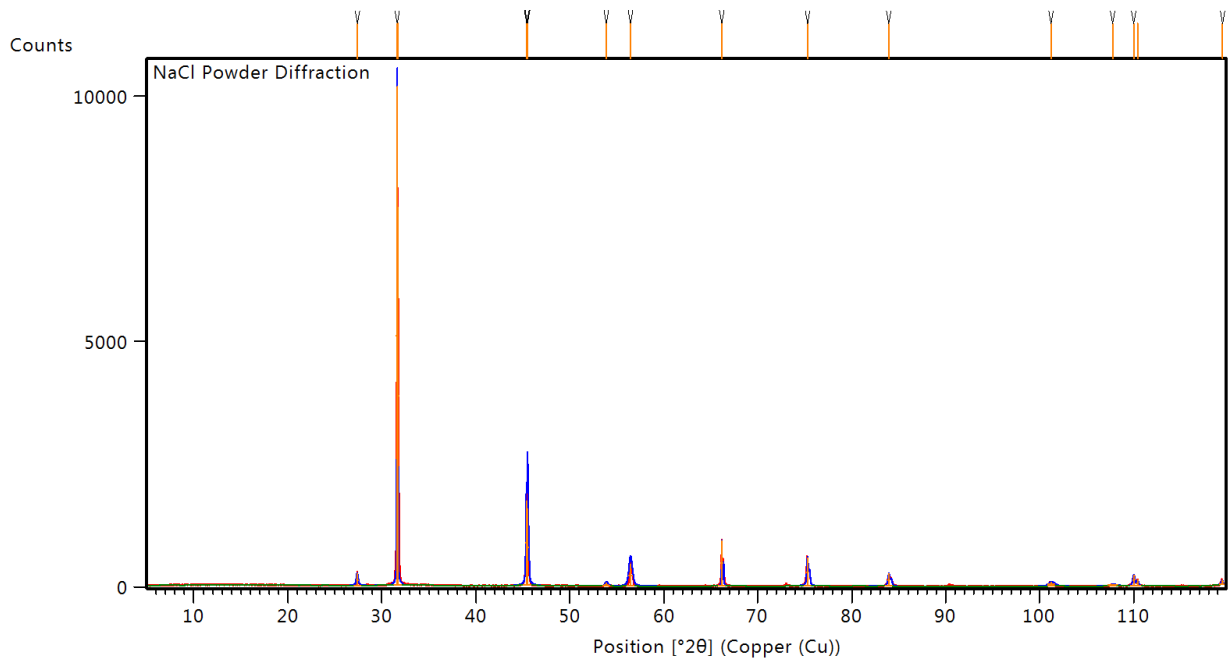


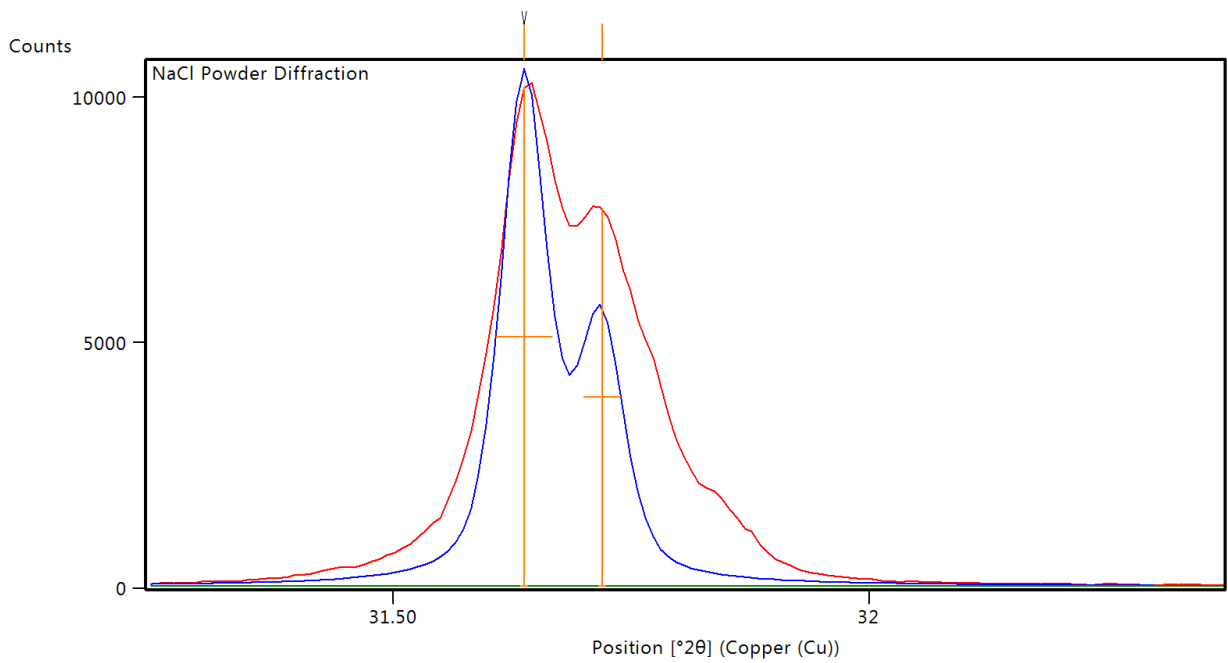
Figure 4: X-rays are generated when collisions with accelerated electrons knock electrons in the copper atoms of the anode out of the K shell. When the electrons fall back to the K shell, X-rays are emitted with energies indicated in [B]. These energy values are important for predicting the X-ray diffraction pattern from Bragg diffraction. [2] [11]

$2\theta$ [°]	Spacing [Å]	Refl. Int. [%]	h	k	l
27.3689	3.25875	2.32	1	1	1
31.6375	2.8258	100	0	0	2
45.3849	1.99671	16.75	0	2	2
53.8732	1.70042	0.58	1	1	3
56.4297	1.6293	4.36	2	2	2
66.1799	1.41092	8.96	0	0	4
75.2911	1.26118	5.54	0	2	4
83.9488	1.15177	2.42	2	2	4

Table 3: Observed peaks from the NaCl sample. Diffraction spacings and the reflected intensity ratios are computed for each located peak. The Miller indices are determined by matching angular position with Table 1. These values are best matches reported by the HighScore software, but uncertainties were not reported. An inspection by eye gives approximately  $\pm 0.05^\circ$  for 98% confidence in the observed angle  $2\theta$ , and the computed standard error for the diffraction spacing is  $\pm 0.20\text{Å}$ .

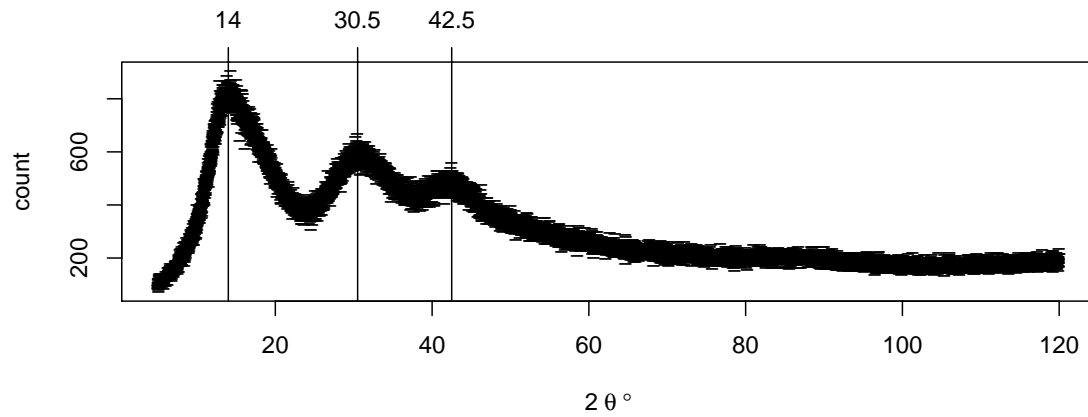


[A]

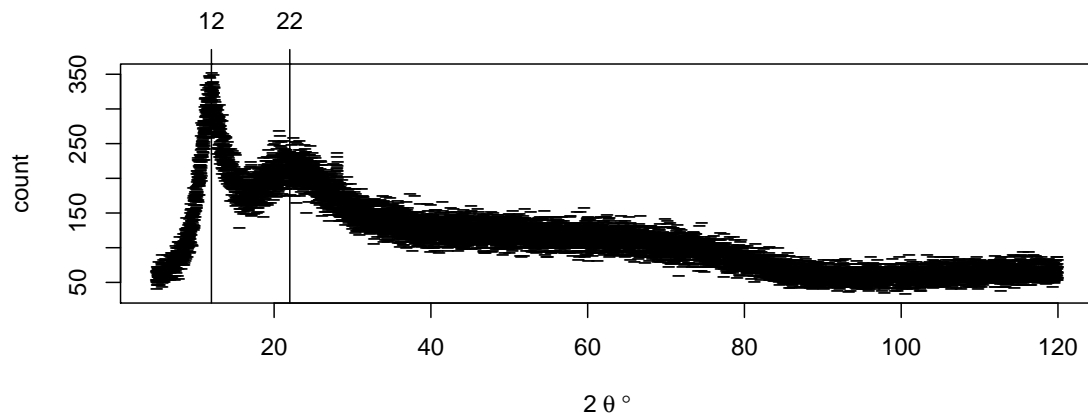


[B]

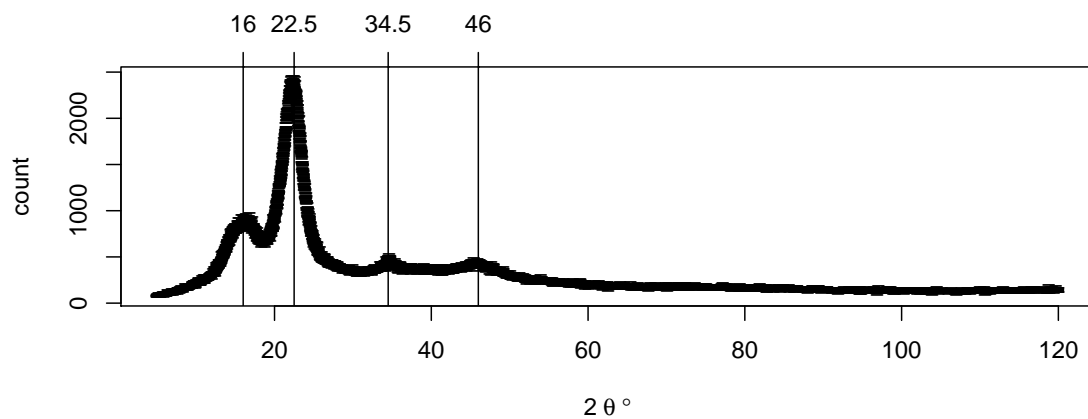
Figure 5: [A] HighScore Plus identified the characteristic NaCl diffraction pattern from Cu K- $\alpha$  and K- $\beta$  emission, and this is used to fit the phase and in turn determine the lattice constant. [B] At the most prominent peak, the detector measurements (red) strongly correlate with the computed diffraction lines (blue).



[A]



[B]



[C]

Figure 6: Diffraction curves observed from the three amorphous samples: [A] unknown plastic; [B] grease; [C] wood. The largest peak should correspond to the average distance between atoms. Secondary peaks may indicate some secondary structure, and an interpretation will be attempted in Section 6.

## 6 Conclusion

### References

- [1] *Bragg diffraction 2*. URL: [https://commons.wikimedia.org/wiki/File:Bragg\\_diffraction\\_2.svg](https://commons.wikimedia.org/wiki/File:Bragg_diffraction_2.svg).
- [2] Clem Burns. *X-ray Diffraction*. Lab Guide. Western Michigan University, Mar. 2017.
- [3] *Carbon*. Apr. 2017. URL: <https://en.wikipedia.org/wiki/Carbon>.
- [4] J.H. Hubbell and S.M. Seltzer. *Tables of X-Ray Mass Attenuation Coefficients and Mass Energy-Absorption Coefficients from 1 KeV to 20 MeV for Elements Z=1 to 92 and 48 Additional substances of Dosimetric Interest*. 1996. URL: <http://www.nist.gov/pml/data/xraycoef/index.cfm>.
- [5] PANalytical. *HighScore Plus Version 4.5*. [www.panalytical.com/Xray-diffraction-software/HighScore/Specifications.htm](http://www.panalytical.com/Xray-diffraction-software/HighScore/Specifications.htm). 2016.
- [6] *PANalytical - Empyrean*. Apr. 2017. URL: <http://www.panalytical.com/Empyrean.htm>.
- [7] *PANalytical - X'Celerator*. Apr. 2017. URL: <http://www.panalytical.com/XCelerator/Specifications.htm>.
- [8] Sarah L. Price. "Predicting crystal structures of organic compounds". In: *Chem. Soc. Rev.* 43 (7 2014), pp. 2098–2111. DOI: 10.1039/C3CS60279F. URL: <http://dx.doi.org/10.1039/C3CS60279F>.
- [9] *Sodium Chloride*. Apr. 2017. URL: [https://en.wikipedia.org/wiki/Sodium\\_chloride](https://en.wikipedia.org/wiki/Sodium_chloride).
- [10] W.E. Wallace and W.T. Barrett. "Studies of NaCl-KCl Solid solutions." In: *Journal of the American Chemical Society* 76 (1954), pp. 366–369. DOI: 10.1021/ja01631a014.
- [11] *X-ray Tube*. URL: <http://www.arpana.gov.au/images/basics/xraytube.png>.

packing fraction for salt, 60% is about good

densities of plastic are all around 2

pick carbon, with occasional oxygens, so using just carbon you get  $2\text{grams}/\text{cm}^3$

[10]

<http://www.chm.bris.ac.uk/webprojects2003/cook/periodicstructures.htm>

for NaCl: penetration depth  $206.156\ \mu\text{m}$  ;  $111.692\ \text{1}/\text{cm}$  linear abs. coeff

for Carbon:  $4462.403\ \mu\text{m}$ ;  $8924.806\ \text{1}/\text{cm}$

383 8872